Brazilian Journal
of Chemical
Engineering

ISSN 0104-6632
Printed in Brazil
www.abeq.org.br/bjche

Vol. 32, No. 01, pp. 201 - 210, January - March, 2015
dx.doi.org/10.1590/0104-6632.20150321s00002820

EVALUATING HYDROGEN PRODUCTION IN BIOGAS REFORMING IN A MEMBRANE REACTOR

F. S. A. Silva*, M. Benachour and C. A. M. Abreu

Department of Chemical Engineering, Federal University of Pernambuco,
CEP: 50740-520, Recife - PE, Brazil.
Phone: + (55) (81) 2126-8901
E-mail: f.aruda@yahoo.com.br

(Submitted: July 1, 2013 ; Revised: February 25, 2014 ; Accepted: April 29, 2014)

Abstract - Syngas and hydrogen production by methane reforming of a biogas (CH_4/CO_2 = 2.85) using carbon dioxide was evaluated in a fixed bed reactor with a Pd-Ag membrane in the presence of a nickel catalyst (Ni 3.31% weight)/γ-Al_2O_3) at 773 K, 823 K, and 873 K and 1.01×10^5 Pa. Operation with hydrogen permeation at 873 K increased the methane conversion to approximately 83% and doubled the hydrogen yield relative to operation without hydrogen permeation. A mathematical model was formulated to predict the evolution of the effluent concentrations. Predictions based on the model showed similar evolutions for yields of hydrogen and carbon monoxide at temperatures below 823 K for operations with and without the hydrogen permeation. The hydrogen yield reached approximately 21% at 823 K and 47% at 873 K under hydrogen permeation conditions.
Keywords: Membrane reactor; Biogas; Methane; Syngas; Hydrogen.

INTRODUCTION

The increasing availability of methane has generated substantial interest in alternative methods for its conversion into synthesis gas (syngas) and/or hydrogen. Research has shown that the catalytic reforming of methane with carbon dioxide (dry reforming) may be employed with natural gas and carbon dioxide emissions rather than traditional methane steam reforming (MSR) for syngas production (Amoro, 1999; Topalidis, 2007; Abreu *et al*., 2008; Silva *et al*., 2012). Major anthropogenic sources of global carbon dioxide emissions include flue gases from coal, oil-fired power stations, thermoelectric plants, FCC refining units, alcoholic fermentation, and several heavy industries, such as those that produce iron, lime, and cement. Biogas, a gaseous mixture of methane and carbon dioxide, can be directly processed by catalytic reforming (Kolbitsch *et al*., 2008; Lau *et al*., 2011). Biogas is produced from organic household waste, industrial waste, and animal dung. Landfill gas is the most important source of biogas because of its relatively high carbon dioxide content (CO_2: 36-41%, CH_4: 48-65%, N_2: 1-17%, and high methane emissions. Qian *et al*. (2002) reported a gas generation rate of 2.50 Nm^3/landfill ton/year for old landfills (> 10 years old). Themelis and Ulloa (2007) estimated a global methane production rate of 75×10^9 Nm^3/year from 1.5×10^9 tons/year of solid landfill, of which only approximately 10% was collected and used.

The expertise developed from the methane dry reforming process (Abreu *et al*., 2008) can be used to increase the production of syngas and hydrogen from biogas. However, thermodynamic constraints and low catalytic performance have been identified as limitations to achieving high methane conversions into

*To whom correspondence should be addressed

hydrogen and carbon monoxide. Operational initiatives of selective product permeation (Garcia-Garcia *et al*., 2013; Faroldi *et al*., 2013; Gallucci *et al*., 2013) can be used to overcome these restrictions when the process is in chemical equilibrium by shifting the composition of the media to increase reactant conversions.

In general, under the same operating conditions, a higher reactant conversion is obtained for reactor operation with permeation using a selective membrane than for a fixed-bed reactor (Kumar *et al*., 2008). Membranes of palladium alloys exhibit a high permeability to hydrogen. Gallucci *et al*. (2008), Shu *et al*. (1991) and Dittmeyer *et al*. (2001) have written reviews on palladium membranes that analyze the effects of permeation on reactor performance.

Kikuchi (1995) demonstrated that the catalytic activity of various metals that were used in a membrane reactor for reforming processes decreased in the following order: Ni>Rh>Pt>Pd>Ru>Ir (alumina support). He used a membrane reactor with a nickel catalyst in methane reforming with carbon dioxide at 773 K and 1.01 MPa to obtain 47% methane conversion versus the 52% conversion predicted by thermodynamic equilibrium calculations. Thus, the high activity of nickel and its low cost make it the best choice for a reforming catalyst, although there is no evidence that it is susceptible to coke formation (Pompeo *et al*., 2007).

This study investigated the activity of a nickel catalyst to convert a biogas via methane reforming with carbon dioxide in order to produce synthesis gas and hydrogen. The process was evaluated in a fixed bed reactor containing a Pd-Ag membrane selective to the permeation of hydrogen and in the presence of the catalyst, in which operations with and without the permeation of hydrogen through the membrane were carried out.

EXPERIMENTAL SECTION

Catalyst Preparation and Characterization

The catalyst was prepared using nickel nitrate ($Ni(NO_3)_2.6H_2O$, Sigma-Aldrich, Germany) and gamma-alumina (γ-Al_2O_3, Degussa, Brazil) via impregnation of alumina with a nickel nitrate solution. First, the impregnated solution was evaporated to dryness. The solid was then dried at 393 K for 12 h and calcinated at 873 K in an argon flow for 5 h. Finally, the catalyst was activated in a hydrogen atmosphere at 973 K for 2 h.

The nickel catalyst was characterized by atomic absorption spectrophotometry (AAS), textural analysis (by the B.E.T. method), and X-ray diffraction (XRD, using CuK-alpha radiation and a Siemens D5000 diffractometer).

Experimental Evaluation

The reforming experiments were performed in a fixed-bed membrane reactor (Figure 1; useful height, $H_R = 45.72\times10^{-2}$ m; outside diameter, $D_R = 1.07\times10^{-2}$ m; Pd-Ag, H_2 selective membrane, height, $H_m = 0.19$ m; inner diameter, $d_m = 0.32\times10^{-2}$m; thickness, $\delta_m = 7.62\times10^{-5}$ m; REB Research & Consulting, USA) with a nickel catalyst ($<d_p> = 412$ μm, $m_{cat} = 0.02\times10^{-1}$ kg) at 773 K, 823 K, and 873 K and 1.01×10^5 Pa. The reactions were investigated with and without hydrogen permeation. A pressure reduction was applied to the internal zone of the membrane under permeation conditions to facilitate hydrogen transfer from the external reaction zone (1.01×10^5 Pa) to the internal zone (0.20 Pa).

The reactants were fed into the reactor with a biogas gaseous mixture of CH_4:CO_2:Ar = 0.89:0.31:1.00 vv at flow rates ranging from 150 to 400×10^{-6} m^3/min (STP).

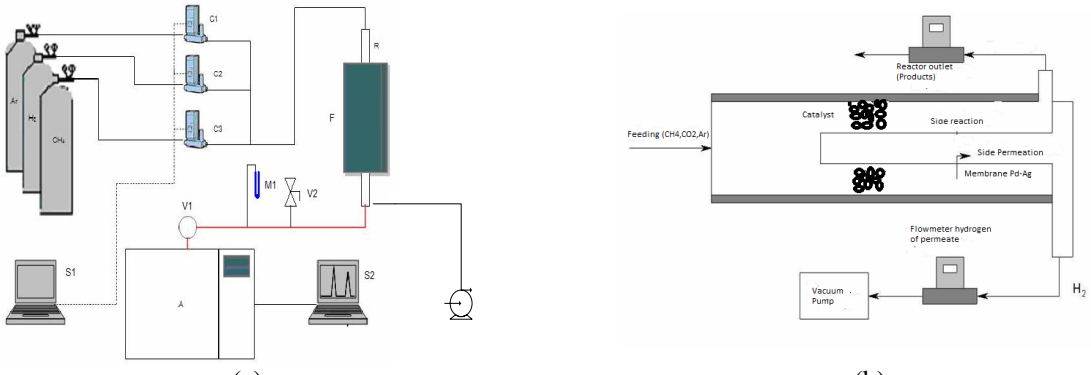

(a) (b)

Figure 1: (a) Scheme of the processing unit of biogas. (A) gas chromatograph, (C1, C2, C3) mass flow meter, (F) Electrical furnace, (R) membrane reactor, (S1) PC computer-mass flow meter control,(S2) PC computer-gas chromatograph, (V1, V2) valves, (M1) U manometer, (E1) vacuum pump, (b) Membrane reactor.

At the top of the reactor, three streams of CH_4, CO_2 and Ar were fed. The residual reagents and products were analyzed using on-line gas chromatography (with a Saturn 2000, Varian, Carbosphere/ Porapak-Q, TCD) of the reactor effluent flow.

After having reached a steady-state regime of processing, the feed stream of methane was stopped while the flows of argon and carbon dioxide were maintained. The residual carbon in the reactor was removed using carbon dioxide via the Boudouard reverse reaction; the effluent gas was analyzed to determine the amount of carbon monoxide produced.

Permeation tests were performed using gaseous mixtures of H_2 and Ar (H_2:Ar:5:50,10:50, 15:50, 20:50, 25:50 v/v*)* at 723 K, 773 K, and 823 K. The results were fitted to the Sieverts equation ($J_{H2} = J_{H20}.\exp(-E_D/RT)[(P_{rH2})^{1/2} - (P_{pH2})^{1/2}]$, Rival *et al*., 2001); to determine the parameters J_{H20} and E_D. Sieverts tests were performed after each reaction experiment to evaluate the state of the membrane.

RESULTS AND DISCUSSION

Catalyst Characterization

The nickel content and the surface areas of the support (pre-treated Al_2O_3) and catalyst (Ni/Al_2O_3) were 3.31% by weight, 226 m^2/g, and 145 m^2/g, respectively, as characterized by AAS and B.E.T.-N_2.

The solid phases of the catalyst used in the reforming reactions were detected by XRD. The γ-Al_2O_3 support was identified at 2θ = 37.4, 45.3, 65.8, and 66.6, and the nickel metallic phase was identified at 2θ = 44.1, 52.0, 77.5, and 93.4. Carbon was found in catalyst samples that were analyzed after the reaction evaluations. Elementary carbon analysis of the used catalyst indicated a carbon content ranging from 0.21% to 0.26% in weight.

Hydrogen Permeation Tests

Experiments on permeation through the selective membrane were conducted in terms of the variables of the Sieverts equation (Figure 2). The permeation rate was investigated as a function of the pressure difference in the membrane at three operating temperatures (723 K, 773 K, and 823 K). The hydrogen permeation rate increased with the H_2/Ar ratio and temperature. Hydrogen permeation experiments (Figure 1(b)) were also performed after the reactions while the system was being cleaned and the catalyst was being regenerated with carbon dioxide (i.e., corresponding to the Boudouard reverse reaction: $CO_2 + C \rightarrow 2CO$).

Figure 2(a) presents the fits to the experimental data using the linear form of the Sieverts equation. These linear fits were used to estimate the following orders of magnitude of the parameters: $J_{H20} = (2.21 \pm 0.41)\times10^{-5}$ mol/m^2s $kPa^{0.5}$ and $E_D = (3.37 \pm 0.13)\times10^3$ J/mol.

Figure 2(b) presents the results of the hydrogen permeation tests that were obtained after regeneration of the catalyst in terms of the variables of the Sieverts equation. For comparison, were also included in this figure the results of the initial tests of permeation at 823 K.

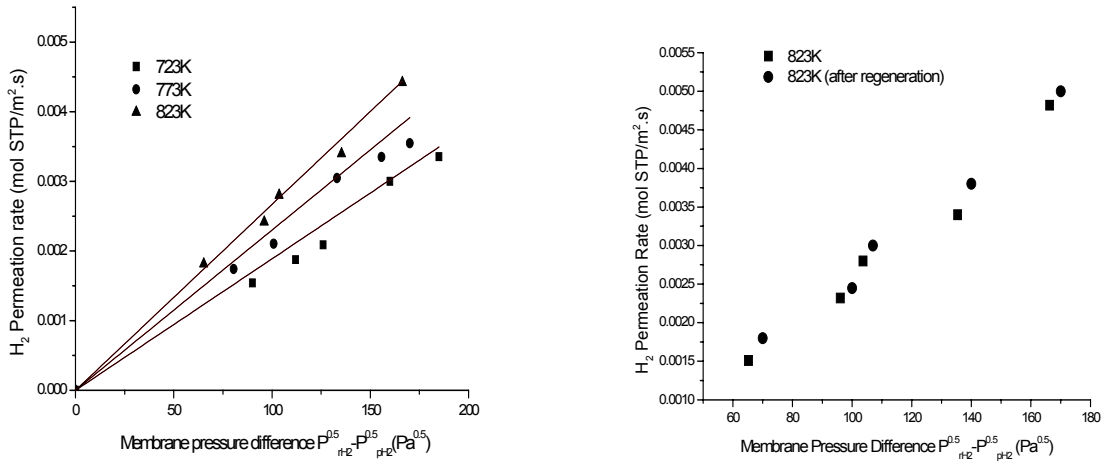

(a) (b)

Figure 2: Permeation rate as a function of the differences between the square roots of pressure in the membrane: (a) effect of temperature and (b) permeation rate after regeneration at an external reaction zone pressure of 1.01×10^5 $Pa^{0.5}$ and an internal zone pressure of 0.20 $Pa^{0.5}$.

Figure 3 presents the carbon dioxide and carbon monoxide concentrations measured during the cleaning/regeneration operation as a function of the time on stream.

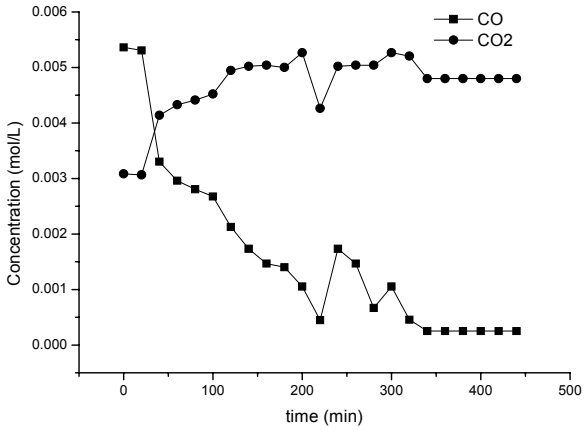

Figure 3: Carbon removal from the membrane reactor. Catalyst and membrane cleaning/regeneration. Conditions: $m_{cat}= 0.02\times10^{-1}$ kg, feed molar ratio $Ar/CO_2 = 1.0$, flow rate = 120 cm^3/min, temperature = 823 K, and pressure = 1.01×10^5 Pa.

The operational performance of cleaning/ regeneration of the membrane reactor, including carbon removal from the catalyst and/or membrane, was determined from the evolution of the reactant and product concentrations in the Boudouard reverse reaction (see Figure 3). After 250 min of operation under a CO_2 stream, the CO level was reduced. In addition, the results of the hydrogen permeation tests (Figure 2(b)) indicated similar system performance before and after the reaction.

Process Evaluation

Experimental evaluations of the reforming process of the biogas were performed in the fixed-bed membrane reactor at three different temperatures (773 K, 823 K, and 873 K) at 1.01×10^5 Pa for a feed gas composition of CH_4:CO_2:Ar = 0.89:0.31:1.00 vv and a spatial time of τ =1,204.8 kg.s/m^3.

The operations were performed in two steps, without and with hydrogen permeation, followed by measuring the component concentrations in the reactor effluents. These experimentally determined concentrations (i.e., the CH_4 and CO_2 conversions and the CO, H_2, and H_2O production) were evaluated over a 4.5-h period. Figure 4 presents the reactant conversions (i.e., $X_i = [Ci_0\text{-}C_i]10^2/Ci_0$, where i = CH_4 and CO_2 and where Ci_0 denotes the initial concentrations) as a function of the time for operation with and without hydrogen permeation at the three temperatures shown. Operations at 823 K and 873 K with H_2 permeation resulted in higher methane conversions than operation without H_2 permeation under the same conditions. The same trend was not observed for the carbon dioxide conversions, which exhibited only a slight increase at higher-temperature operation. The permeation effect occurred during the reaction step in the methane cracking process, shifting the reaction equilibrium such that the conversion of methane to hydrogen was increased. The carbon dioxide concentrations remained largely unchanged.

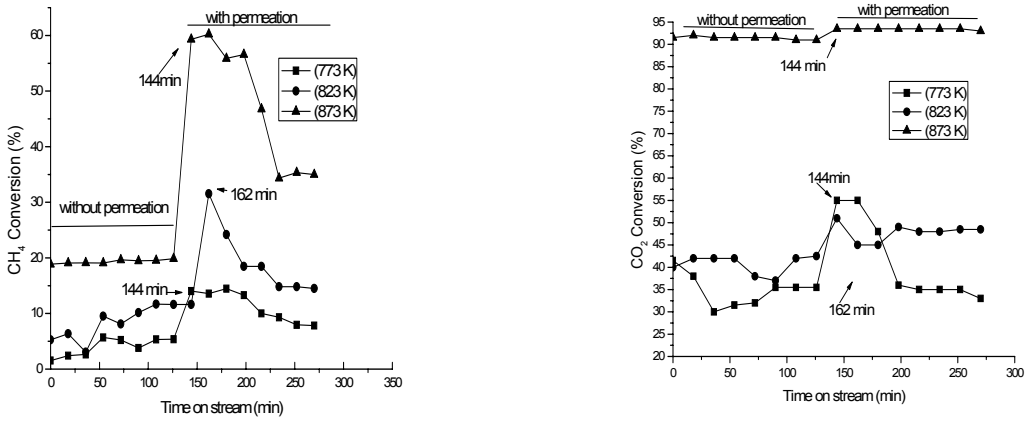

(a) (b)

Figure 4: Reactant conversions for (a) CH_4 and (b) CO_2 as a function of time for operations in a membrane reactor illustrating the effects of temperature under the following conditions: catalyst Ni (3.31% weight)/γ-Al_2O_3, $m_{cat} = 0.02 \times 10^{-1}$ kg, feed molar ratio $CH_4/CO_2 = 2.85$, and τ = 1,204.8 kg.s/m^3 at a pressure of 1.01×10^5 Pa.

Figure 4 illustrates that initiating hydrogen removal by permeation significantly increased the methane conversion at the two highest temperatures. In the stages following the permeation step, higher steady-state methane conversions were attained than for operation without permeation.

Figure 5 presents the hydrogen and carbon monoxide yields ($Y_j = [C_j/\Sigma C_{i0}] \times 10^2$), j = CO and H_2) for the process. The hydrogen production increased for operation with H_2 permeation at 823 K and 873 K, whereas the carbon monoxide level remained steady.

Tables 1 and 2 provide the experimental conversions and yields obtained under steady-state conditions at the three temperatures considered.

Under hydrogen permeation at 873 K, the methane conversion increased by 83% and the hydrogen yield was approximately 113% higher compared to operation without permeation. Galuszka *et al*. (1998) obtained a methane conversion of 48.6% and a hydrogen yield of 46.5% using a nickel catalyst in a membrane reactor under the same conditions as this study.

Although the effects of the operating conditions (i.e., the feed flow rate, feed ratio, temperature, pressure, and catalyst weight) on the CH_4 and CO_2 conversions should be considered, the biogas conversion in a membrane reactor is generally expected to be greater than that in a fixed-bed reactor.

Munera *et al*. (2003) evaluated the methane dry reforming process in a membrane reactor (with a Pd/Ag membrane) using a 0.6% weight Rh/Al_2O_3 catalyst at 823 K and atmospheric pressure. The study obtained methane and carbon dioxide conversions of 33.9% and 41%, respectively, for a feed molar ratio of $CH_4/CO_2 = 1.0$. The methane and carbon dioxide conversions obtained in the present study were 14.5% and 48%, respectively, under the same conditions. The lower methane conversion may be attributed to the applied feed molar ratio ($CH_4/CO_2 = 2.85$) of the biogas.

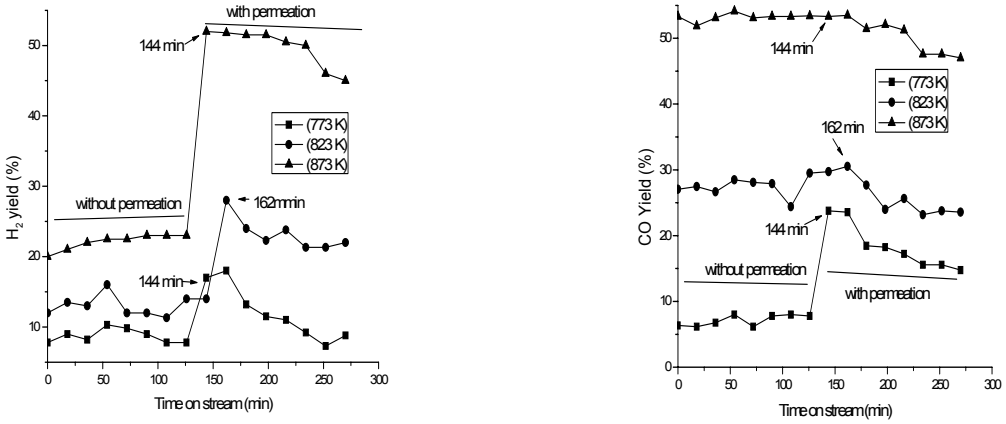

(a) (b)

Figure 5: Product yield for (a) H_2 and (b) CO as a function of time for operation in a membrane reactor illustrating the effects of temperature under the following conditions: catalyst, Ni (3.31% weight)/γ-Al_2O_3, $m_{cat} = 0.02 \times 10^{-1}$ kg, feed molar ratio $CH_4/CO_2 = 2.85$, and $\tau = 1{,}204.8$ kg.s/m^3 at a pressure of 1.01×10^5 Pa.

Table 1: Component conversions of the biogas reforming process in a membrane reactor at the following steady-state conditions: Ni (3.31% weight)/γ-Al_2O_3, $m_{cat} = 0.02 \times 10^{-1}$ kg, feed molar ratio $CH_4/CO_2 = 2.85$, and $\tau = 1{,}204.8$ kg.s/m^3 at a pressure of 1.01×10^5 Pa.

Temperature (K)	Conversion (%) without permeation		Conversion (%) with permeation	
	CH_4	CO_2	CH_4	CO_2
773	4.61	35.11	7.79	34.09
823	11.53	42.56	14.54	48.16
873	19.25	92.61	35.33	92.87

Table 2: Product yields for the biogas reforming process in a membrane reactor under the following steady-state conditions: catalyst Ni (3.31% weight)/γ-Al_2O_3, $m_{cat} = 0.02 \times 10^{-1}$ kg, feed molar ratio $CH_4/CO_2 = 2.85$, and $\tau = 1{,}204.8$ kg.s/m^3 at a pressure of 1.01×10^5 Pa.

Temperature (K)	Yield (%) Without permeation		Yield (%) with permeation	
	H_2	CO	H_2	CO
773	7.52	7.14	9.23	15.41
823	15.49	30.06	21.14	25.22
873	22.80	53.21	47.00	46.82

The experimental results for biogas reforming in this comparative evaluation were explained using a set of reaction mechanisms for the reforming process developed by Abreu *et al*. (2008) for the same catalyst, which consisted of the following major reaction steps: methane catalytic cracking, with carbon deposition and hydrogen production (I: $CH_4 \leftrightarrow C + 2H_2$); hydrogen consumption via a water gas-shift reverse reaction (II: $CO_2 + H_2 \leftrightarrow CO + H_2O$); and carbon consumption by carbon dioxide (III: $CO_2 + C \leftrightarrow 2CO$, i.e., the Boudouard reverse reaction). Thus, in operation with hydrogen permeation, the methane conversion increased to maintain the methane catalytic cracking equilibrium (step I). Accordingly, the removal of hydrogen from the reaction medium delayed the reverse water gas-shift reaction (step II), decreasing the carbon dioxide consumption. Therefore, the available carbon dioxide partially cleaned the carbon deposited on the catalyst (step III), maintaining the activity level of the nickel catalyst during the process.

Kinetic and Reactor Modeling

The relations r_{ji} (j = I, II, III), which correspond to the rate laws of the reaction steps of the biogas reforming process, were expressed as follows:

$$r_{ICH4} = \frac{k_1 K_{CH_4} C_{CH_4}}{1 + K_{CH_4} C_{CH_4}} \quad (1)$$

$$r_{IICO_2} = k_2 (C_{H_2} C_{CO_2} - \frac{C_{CO} C_{H_2O}}{K_{eqwgs}}) \quad (2)$$

$$r_{IIICO_2} = k_3 C_{CO_2} \quad (3)$$

The global reaction rates of each component (r_i; i = CH_4, CO_2, CO, and H_2O) were written as follows:

$$r_{CH_4} = -r_{ICH_4};\ r_{CO_2} = -(r_{IICO_2} + r_{IIICO_2}) \quad (4)$$

$$r_{CO} = r_{IICO_2} + 2r_{IIICO_2};$$
$$r_{H_2} = 2r_{ICH_4} - r_{IICO_2};\ r_{H_2O} = r_{IICO_2} \quad (5)$$

The evolution of the effluent concentrations for the membrane reactor was obtained from mass balances incorporating component reaction rates based on the three aforementioned reaction steps. In the mass balance equation a constant flow rate along the reactor was considered based on the experimental conditions employed (biogas mixture diluted in argon, with low content in carbon dioxide, and operations with low methane conversions).

The resulting differential equations were expressed as $dC_i/d\tau + r_i = 0$, where τ (kg.s/m^3) was the modified spatial time. The differential equation for the mass balance of hydrogen for the permeation operation was as follows:

$$-\frac{dc_{H_2}}{d\tau} - S_m \frac{j_0 e^{-E_D/RT}}{}(\sqrt{C_{H2}.R.T} - \sqrt{P^p_{H2}}) + r_{H_2} = 0 \quad (6),$$

where $S_m = A_m/m_{cat} = (4d_m.[(D_R^2 - d_m^2)\rho_{cat}(1-\varepsilon)]^{-1})$ is the ratio between the membrane surface area and the mass of the catalyst and ε denotes the bed porosity. The corresponding initial conditions ($\tau = \tau_0$) were as follows:

$$C_{CH_4}(\tau_0) = C_{CH_{4o}};\ C_{CO_2}(\tau_0) = C_{CO_{2o}};$$
$$C_{CO}(\tau_0) = C_{H_2}(\tau_0) = C_{H_2O}(\tau_0) = 0.$$

The isothermal conditions of the operations were guaranteed by the feed, the convective heat discharge, the heat released with hydrogen permeation, the reaction enthalpies ($\Delta H_J.r_{Ji}$), and the heat transferred from the oven through the reactor wall. The thermal behavior of the reactive operations was modeled by a steady-state energy balance incorporating the aforementioned effects. The following differential equation (Equation (7)) describes the temperature evolution as a function of the modified spatial time:

$$\rho_{pM}.\rho_g \frac{dT}{d\tau} = -(\Delta H_I r_{CH4} + \Delta H_{II} r_{CO2} + \Delta H_{III} r_{CO2}) - \frac{4U}{d_R.\rho_{cat}}(T - T_{RE}) - \frac{S_m}{\rho_{H2}} \frac{d_m}{D_R}(1 - \delta_{H2}) J_{H2}(H_{rH2} - H_{mH2});$$
$$T(\tau_0) = T_0 \quad (7)$$

where ρ_g = 15.28 mol/m^3, U (the overall heat transfer coefficient) = 2.41 J/m^2.s.K, $D_R = 1.07 \times 10^{-2}$ m, ρ_{cat} = 1,200 kg/m^3, and ρ_{H2} = 71 kg/m^3. The reformer and sweep gas enthalpy are denoted by H_{rH2} and H_{mH2}, respectively. The temperature $T_{RE} = T_0 = 750$ K and $Cp_M = 29.30 + 0.023T - 8.96x10^{-6}T^2 - 1.40x10^{-9}T^3$ J/mol.K, where C_{pM} denotes the heat capacity of the mixture of CH_4, CO_2, and Ar. The enthalpies of re-

action can be expressed in the following form: $\Delta H_J = \int_{To}^{T} \sum \nu_i C_{PJ} dT; C_{PJ} = a_i + b_i T + c_i T^2$.

The mass balance equations and Equation 7 were solved for the effluent concentrations and the temperature of the reaction medium using the fourth-order Runge-Kutta method. The values of the kinetic and adsorption parameters were estimated from our previous work (Abreu *et al*., 2008). The Arrhenius and van't Hoff correlations were expressed as follows:

- methane cracking reaction: $k_1 = 3.58\times10^{9}\exp(-248.55/RT)$ mol/kg.s and $K_{CH4} = 31.39\times10^{-11}\exp(167.32/RT)$ m^3/mol;

- water gas-shift reverse reaction: $k_2 = 1.07\times10^{13}\exp(-350.08/RT)$ $(m^3)^2$/mol/kg.s; and

- carbon dioxide-carbon interaction (i.e., the Boudouard reverse reaction): $k_3 = 1.16\times10^{5}\exp(-115.86/RT)$ m^3/kg.s.

The equilibrium constant of the water gas-shift reaction was given as follows:

$$K_{eqwgs} = \exp(-6.31x10^{-2} - 1.86x10^{-7}\ln(T) + 2.11x10^{-4}T + 9.37x10^{-4}T^{-1} - 5.44x10^{-6}(T-298.15)T^{-2}) \quad (8)$$

The component concentrations at the reactor exit were calculated as a function of the temperature over the 750-895 K range for operations with and without hydrogen permeation under different steady-state conditions. The experimental results obtained under steady-state conditions at 773 K, 823 K, and 873 K (see Figures 6 and 7) are shown on the same graph for comparison with the predictions.

Figures 6 and 7 illustrate that the experimental component concentrations exhibited the same trends predicted by the model equations, except for hydrogen concentrations at temperatures higher than 823 K (Figure 7(a)). The concentrations of carbon dioxide and carbon monoxide in the output gas were similar with and without the permeation of hydrogen. However, the concentrations of methane and hydrogen were approximately 23% and 51% lower, respectively, when the system operated with permeation. Methane was further consumed to maintain the equilibrium, which was temporarily displaced by hydrogen permeation. The small amount of available hydrogen in the reaction medium could be processed by the water gas shift reverse reaction (step II). Thus, residual carbon dioxide, not consumed by the reaction with hydrogen, was used to process the carbon into carbon monoxide by the Boudouard reverse reaction (step III).

The predicted component concentrations had approximate values at temperatures lower than 823 K for operations with and without hydrogen permeation. When hydrogen permeation was used, lower methane, carbon monoxide and hydrogen concentrations were predicted in the reactor effluent gas for temperatures above 823 K.

Figure 8 presents the model predictions and the evolution of the carbon monoxide and hydrogen yields ($Yj = [Cj/\ \Sigma Ci_0] \times 10^2$, where j = CO and H_2) with and without hydrogen permeation ($C_{H2} = C_{H2permeated} + C_{H2reactor\ exit}$). The hydrogen yield was

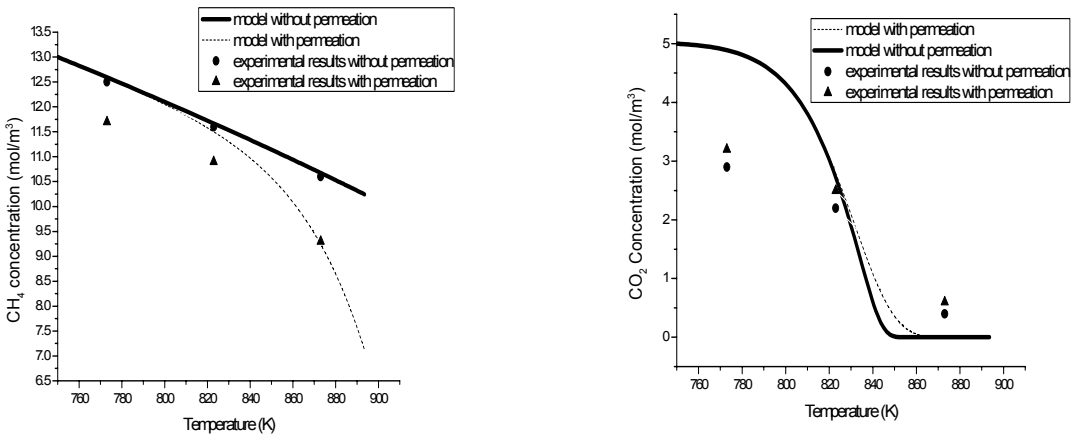

Figure 6: Model predictions and experimental concentrations as a function of temperature for steady-state operation with and without hydrogen permeation for methane-carbon dioxide biogas reforming in a membrane reactor for reactants (a) CH_4 and (b) CO_2, under the following operating conditions: $m_{cat} = 0.02 \times 10^{-1}$ kg, $P = 1.01 \times 10^5$Pa, $CH_4/\ CO_2 = 2.85$, and $\tau = 1{,}204.8$ kg.s/m^3.

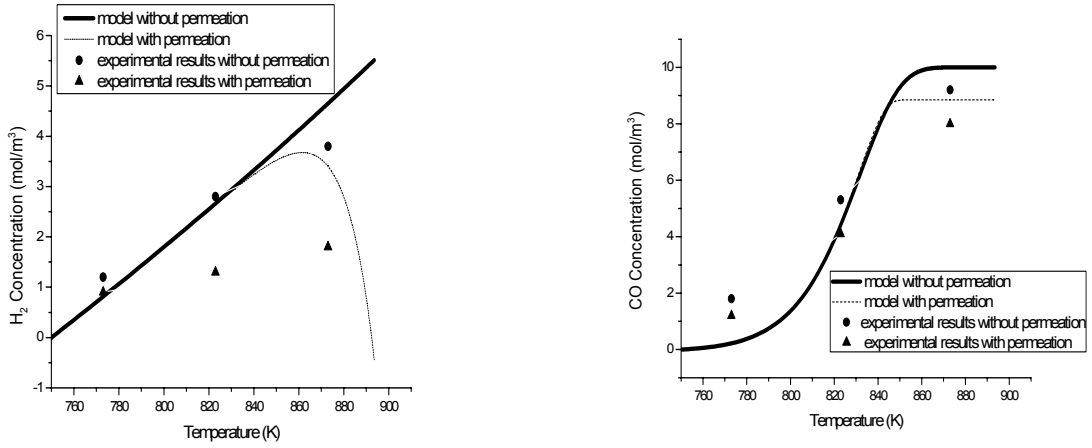

(a) (b)

Figure 7: Model predictions and experimental concentrations as a function of temperature for steady-state operation with and without hydrogen permeation for methane-carbon dioxide biogas reforming in a membrane reactor, showing products (a) H_2 and (b) CO under the following operating conditions: $m_{cat} = 0.02 \times 10^{-1}$ kg, $P = 1.01 \times 10^5$ Pa, $CH_4/CO_2 = 2.85$, and $\tau = 1{,}204.8$ kg.s/m^3.

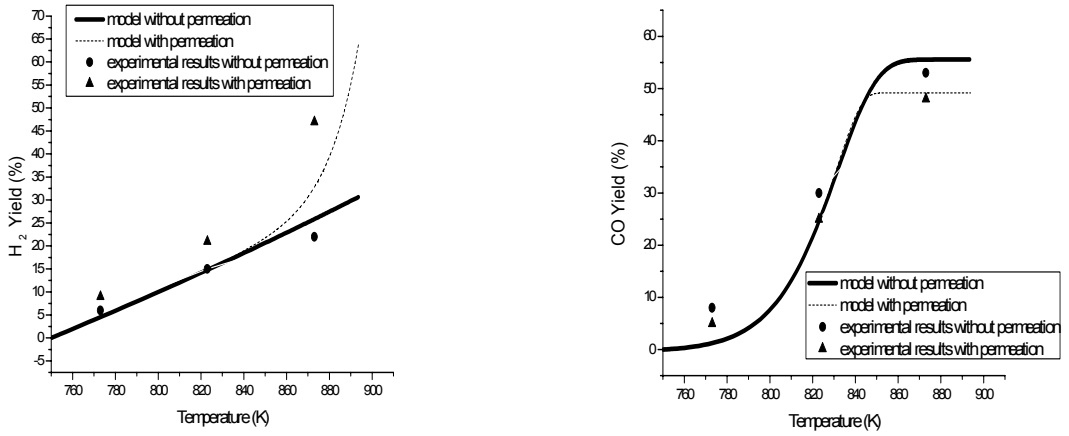

(a) (b)

Figure 8: Model predictions and experimental product yields for (a) H_2 and (b) CO for operations with and without hydrogen permeation for methane-carbon dioxide reforming in a membrane reactor under the following operating conditions: $m_{cat} = 0.02 \times 10^{-1}$ kg, $P = 10.1 \times 10^5$ Pa, $CO_2/CH_4 = 0.35$, and $\tau = 1{,}204.8$ kg.s/m^3.

predicted to increase strongly with the temperature and more so for operation with permeation. A higher carbon monoxide yield was predicted for operation without permeation than with permeation at 873 K.

An increased sensitivity to thermal effects was predicted using Sieverts equation for hydrogen mass transfer by permeation for operation at temperatures above 840 K. Thus, hydrogen permeation increased rapidly for operations at temperatures above 840 K, and the hydrogen production (Figure 8(a)) increased via methane cracking.

CONCLUSIONS

A fixed-bed reactor with a Pd-Ag/H_2 selective membrane was used to convert biogas into syngas by a reforming process. The performance of a nickel catalyst (3.31% weight)/γ-Al_2O_3) was evaluated at 773 K, 823 K, and 873 K and 1.01×10^5 Pa with and without hydrogen permeation. Operation with permeation at 873 K increased the biogas methane conversion to approximately 83%, and the hydrogen yield was 113% higher than that for operation without hydrogen permeation.

A mathematical model was formulated to predict the evolution of the effluent concentrations of the membrane reactor as a function of the operating temperature. At temperatures lower than 823 K, similar evolution profiles were predicted for the hydrogen and carbon monoxide yields for operations with and without hydrogen permeation. The hydrogen yield reached approximately 21% at 823 K and 47% at 873 K under hydrogen permeation conditions.

ACKNOWLEDGMENTS

The authors acknowledge the financial support provided by CAPES, FINEP, and PETROBRAS, Brazil for this study.

NOTATIONS

A	Membrane area	m^2
C	Concentration	mol/m^3
Cp	Heat capacity	J/mol.K
d_m	Inside membrane diameter	m
D_R	Outside reactor diameter	m
dp	Catalyst pore diameter	μm
E_D	Diffusivity activation energy	J/mol
h_m	Membrane height	m
H_R	Reactor height	m
J_{H2}	Permeation flux	$mol/m^2.s$
J_{H20}	Pre-exponential factor for permeation flux	$mol/m^2.s.Pa^{0.5}$
k_1	Kinetic constant for the step I reaction	mol/kg.s
k_2	Kinetic constant for the step II reaction	$(m^3)^2/mol.kg.s$
k_3	Kinetic constant for the step III reaction	$m^3/kg.s$
K_{CH4}	Adsorption equilibrium constant of methane	m^3/mol
K_{eqwgs}	Equilibrium constants for the RWGS reaction	(-)
K_{eqCH4}	Equilibrium constants for the methane decomposition reaction	(-)
m	Catalyst mass	kg
P	Pressure	Pa
r_{ji}	Rate of consumption/ production of component	mol/kgcat.s
R	Gas constant	J/mol.K
S_{BET}	Specific surface area	m^2/g
T	Temperature	K
U	Overall heat transfer coefficient	$J/s.m^2.K$
X	Conversion	%
Y	Yield	%

Greek Letters

ε	Bed porosity	(-)
ρ	Density	kg/m^3
ρ_g	Density of gaseous mixture	kg/m^3
τ	Spatial time	$kg/s.m^3$
γ	Gamma	(-)
Δ H	Heat of reaction	J/mol
δ_m	Thickness	m

Suffix

i	Components (CH_4, CO_2, CO, H_2, and H_2O)
j	Reaction steps
r_{H2}	Hydrogen from reaction side
p_{H2}	Hydrogen partial pressure from permeation side
R	Reactor
RE	Reference
cat	Catalyst
M	Mixture !

REFERENCES

Abreu, C. A. M., Santos, D. A., Pacífico, J. A., Filho, N. M. L., Kinetic evaluation of methane-carbon dioxide reforming process based on the reaction steps. Ind. Eng. Chem., 47, p. 4617-4622 (2008).

Amoro, J. N., The multiple roles for catalysis in production of H_2. Appl. Catal. A: Gen., 176, p. 159-176 (1999).

Dittmeyer, R., Volker, H., Daub, K., Membrane reactors for hydrogen and dehydrogenation process based on supported palladium. J. Mol. Catal. A: Chem., 173, p. 135-184 (2001).

Faroldi, B., Bosko, M. L., Múnera, J., Lombardo, E., Cornaglia, L., Comparison of $Ru/La_2O_2CO_3$ performance in two different membrane reactors for hydrogen production. Catal. Today, 213, p. 135-144 (2013).

Gallucci, F., Fernandez, E., Corengia, P. and van Sint Annaland, M., Recent advances on membranes and membrane reactors for hydrogen production. Chemical Engineering Science, 92, p. 40-66 (2013).

Gallucci, F., Tosti, S., Basile, A., Pd–Ag tubular membrane reactors for methane dry reforming: A reactive method for CO_2 consumption and H_2 production. Journal of Membrane Science, 317, p. 96-105 (2008).

Galuszka, J., Pandey, R. N., Ahmed, S., Methane-conversion to syngas in a palladium membrane reactor. Catal. Today, 46, p .83-89 (1998).

García-García, F. R., Soria, M. A., Mateos-Pedrero, C., Guerrero-Ruiz, A., Rodríguez Ramos, I., Li, K., Dry reforming of methane using Pd-based membrane reactors fabricated from different substrates. Journal of Membrane Science, 435, p. 218-225 (2013).

Kikuchi, E., Palladium/ceramic membranes for selective hydrogen permeation and their application to membrane. Catal. Today, 25, p. 333-337 (1995).

Kolbitsch, P., Pfeifer, C., Hofbauer, H., Catalytic steam reforming of model biogas. Fuel, 87, p. 701-706 (2008).

Kumar, S., Agrawal, M., Kumar, S., Jilani, S., The production of syngas by dry reforming in membrane reactor using alumina-supported Rh catalyst: A simulation study. J. Chem. React. Eng., 6, A-109, p. 1-39 (2008).

Lau, C. S., Tsolakis, A., Wyszynski, M. L., Biogas upgrade to syn-gas (H_2–CO) via dry and oxidative reforming. Int. J. Hydrogen Energ., 36, p. 397-404 (2011).

Munera, J., Irusta, S., Cornaglia, L., Lombrado, E., CO_2 reforming of methane as a source of hydrogen using a membrane reactor. Appl. Catal. A: Gen., 245, p. 383-395 (2003).

Pompeo, F., Nichio, N. N., Souza, M. M. V. M., Cesar, D. V., Ferretti, O. A., Schmal, M., Study of Ni and Pt catalysts supported on $\alpha - Al_2O_3$ and ZrO_2 applied in methane reforming with CO_2. Appl. Catal. A: Gen., 316, p. 175-183 (2007).

Qian, X., Koerner, R. M., Gray, D. H., Geotechnical Aspects of Landfill Design and Construction. First Ed., Prentice Hall, New York (2002).

Rival, O., Grandjean, B. P. A., Guy, C., Sayari, A., Larachi, F., Oxygen-free methane aromatization in a catalytic membrane reactor. Kinet. Catal. React. Eng., 40, p. 2212-2219 (2001).

Shu, J., Grandjean, B. P. A., Van Neste, A., Kaliaguine, S., Catalytic palladium based membrane reactors: A review. Can. J. Chem. Eng., 69, p. 1036-1060 (1991).

Silva, F. A., Hori, C. E., da Silva, A. M., Mattos, L. V., Munera, J., Cornaglia, L., Noronha, F. B., Lombardo, N. E., Hydrogen production through CO_2 reforming of CH_4 over $Pt/CeZrO_2/Al_2O_3$ catalysts using a Pd–Ag membrane reactor. Catal. Today, 193, p. 64-73 (2012).

Themelis, N. J., Ulloa, P. A., Methane generation in landfills. Renew. Energ., 32, p. 1243-1257 (2007).

Topalidis, A., Petrakis,D. E., Ladavos, A., Loukatzikou, L., Pomonis,P. J., A kinetic study of methane and carbon dioxide interconversion over 0.5%Pt/ SrTiO3 catalysts. Catal. Today, 127, p. 238-245 2007).